

# Apparent equation of state of compact stars within the Eddington-inspired Born-Infeld theory

A. I. Qauli<sup>1</sup> A. Sulaksono<sup>1</sup> H. S. Ramadhan<sup>1</sup> I. Husin<sup>2</sup>

<sup>1</sup>Departemen Fisika, FMIPA, Universitas Indonesia, Depok 16424, Indonesia.

<sup>2</sup>Theoretical Physics Lab., THEPI Division, Institut Teknologi Bandung, Jl. Ganesha 10 Bandung 40132, Indonesia.

E-mail: [ali.ikhsanul@sci.ui.ac.id](mailto:ali.ikhsanul@sci.ui.ac.id), [anto.sulaksono@sci.ui.ac.id](mailto:anto.sulaksono@sci.ui.ac.id), [hramad@ui.ac.id](mailto:hramad@ui.ac.id), [idrushusin@students.itb.ac.id](mailto:idrushusin@students.itb.ac.id)

**Abstract.** The compactness of realistic neutron stars (NSs) and quark stars (QSs) within the Eddington-inspired Born-Infeld (EiBI) theory of gravity and the energy conditions of the corresponding apparent equation of states (EOSs) are investigated. We have shown that the maximum compactness constraint extracted from the recent pulsars masses and radii observations can provide the upper limit of EiBI  $\kappa$  value. By using extended relativistic mean field (ERMF) model to describe NS core EOS including hyperons, it can be estimated that  $\kappa_g^{\max} \approx 7.9 \times 10^{-2} \text{m}^5 \text{kg}^{-1} \text{s}^{-2}$ . If we use confined-isospin-density-dependent-mass (CIDDm) model with additional vector Coulomb term to describe QS EOS, we can obtain lesser value i.e.,  $\kappa_g^{\max} \approx 2.2 \times 10^{-2} \text{m}^5 \text{kg}^{-1} \text{s}^{-2}$ . We have also observed that for large  $\kappa$  values, mass-radius relations of NSs and QSs do not exceed causality restrictions because the compactness of NS and QS are saturated after passing certain large critical value. This observation is in agreement with the results obtained in Ref.[1] for the case of pressure-less stars. We have also found that if  $\kappa \geq$  certain non-zero value, the CIDDm with vector Coulomb model prediction of QS can reach the maximum mass  $\gtrsim 2 M_\odot$ . It is also shown that the corresponding apparent EOS of NSs and QSs can satisfy the energy conditions. However, in the NSs case, the square of the sound speed of the corresponding apparent EOSs in the near-surface region is negative. There is also indication that the strong energy condition can be violated by NS and QS EOSs. However it can be happen only when  $\kappa$  is extremely large. In general, physical requirements for acceptable interior solution for static fluid spheres of GR can be also violated by apparent EOS.

---

## Contents

<b>1</b>	<b>Introduction</b>	<b>1</b>
<b>2</b>	<b>Formalism</b>	<b>3</b>
2.1	EiBI theory as GR with apparent EOS	3
2.2	Compact stars in EiBI theory	8
<b>3</b>	<b>Results and discussion</b>	<b>9</b>
<b>4</b>	<b>Conclusion</b>	<b>11</b>

---

## 1 Introduction

Einstein’s general relativity (GR) theory has solid conceptual foundation and it passes all precision test for intermediate energy scales with flying colors. However, on cosmological scale GR also faces problems such as the need of dark energy and dark matter. The theoretical and experimental indications of modification of GR at small and large energies are reviewed in Refs. [2–4]. In compact stars such as NSs and Qs, gravity plays a relatively dominant role and its collapse leads to large-curvature and strong-gravity environments [2, 4]. Therefore, the differences in predictions between GR and alternative or modified gravity theories could appear significantly [5, 6]. On the other hand, even though significant progress has been reported, until now the equation of state (EOS) of a NS is still uncertain (see Refs. [7–13] and the references therein). Similarly, the QS EOS is also model-dependent [14–20]. It is, however, worthy to note that recently there are some studies about an EOS-independent relation of some NS properties such as moment of inertia, Love number and quadrupole moment as well as the relation of other multiple moments [21–23].

Among GR modified theories, the Eddington-inspired Born-Infeld (EiBI) theory attracts quite a lot attentions recently due to its distinctive features compared to those of GR (see details in Refs. [1, 24–26] and the references therein). The theory, proposed by Banados and Ferreira [27] fusing Palatini approach, is a gravitational analog of a nonlinear theory of electrodynamics known as the Born-Infeld theory [2, 4, 28]. The reviews of the investigations and applications of EiBI theory can be found in Ref. [2] and the references therein. While the most recent comprehensive review of general Born-Infeld inspired modifications of gravity theories and their applications can be found in Ref. [24].

However, we need to note some features of EiBI theory related to this work. The authors of Refs. [25, 29–31] have shown that the Tolman-Oppenheimer-Volkov (TOV) equation version obtained by using EiBI theory could increase or decrease the maximum mass of NS by adjusting the corresponding  $\kappa$  value. The author of Ref. [31] has also found that through direct observations of the NS radii around  $0.5 M_{\odot}$  and the precise measurements of neutron skin thickness of  $^{208}\text{Pb}$ , the EiBI theory could be discriminated from GR. Furthermore, it is also reported that the range of reasonable values of  $\kappa$  parameter in EiBI theory can be constrained by using some astrophysical and cosmological data [32], NSs properties [25, 26, 29, 33] and the Sun properties [34]. The possibility for distinguishing EiBI theory from GR is also suggested by observing gravitational wave from NS (see Ref. [35] for details). Concerning the stellar stability of EiBI theory, the authors of Ref. [36] has shown that the standard results of stellar

stability still hold in EiBI theory where for a sequence of stars with the same EOS, the fundamental mode  $\omega^2$  passes through zero at central density corresponding to the maximum-mass configuration is similar to the one found in GR. Therefore, the corresponding point marks the boundary of the onset of instability where the stellar models with central densities less than the corresponding critical points are stable. Furthermore, The authors of Ref. [26] have also shown that there always exists regular solution for compact stars with  $\kappa > 0$  and the corresponding stars have maximum compactness of  $\frac{GM}{R} \sim 0.3$  which is roughly independent from  $\kappa$ . The collapse constraint, i.e., the compact stars exist if the requirement  $\kappa\Delta < 0$  is satisfied, with  $\Delta$  is

$$\Delta = (P_c\kappa - 3\kappa\rho_c - 4)(1 + \kappa\rho_c) - \kappa(1 - \kappa P_c)(P_c + \rho_c)\frac{d\rho(P_c)}{dP_c},$$

here  $P_c$  and  $\rho_c$  are the central pressure and density of the stars. It means that if the EOS is thermodynamically consistent, the onset of the star stability region in EiBI theory depends only on  $P_c$  and  $\kappa$ . We also need to note that the EiBI theory shows also a singularity associated with the phase transition matter for negative  $\kappa$  due to the appearance of discontinuity in energy density around transition region [37]. The curvature singularities appearing at surface of compact stars within EiBI theory for polytropic EOS have been already discussed for examples in Refs. [38–41].

In the case when the matter of the star can be described by an ideal fluid with barotropic EOS, the modified field equations within EiBI with physical EOS (The ideal fluid energy-momentum tensor is derived from the microscopic interaction among the constituents of the corresponding matter) can exactly also be expressed as field equations of GR but with effective ideal fluid energy-momentum tensor. The corresponding EOS has highly nonlinear relation between the pressure and the energy density. This EOS is called the apparent EOS in Ref. [1]. The observations like NSs as well as other compact object properties are difficult to distinguish this degeneracy [1, 2]. It is interesting that even the EOS of matter in flat space time satisfies all energy conditions, but the apparent EOS could violate strong energy condition (SEC) or real  $\tau$  condition of EiBI theory. The corresponding violation is demonstrated in Ref. [1] in the case of dust (pressureless) EOS. Note that the most important matter properties in GR encoded in various energy conditions which have some physical consequences (see details in Ref. [1] and references therein) and furthermore, the EOS is also restricted by some requirements in order the interior solution for static fluids spheres of GR to be physically meaningful [30]. Therefore, it is also quite tempting to check whether the fulfilling of energy conditions and internal solution requirements of the apparent EOS can be used to obtain theoretically acceptable upper limit of  $\kappa$ . This corresponding upper limit can not be obtained directly from the modified field equations within EiBI with physical EOS point of view. Note that the upper limit of  $\kappa$  is defined as the largest  $\kappa$  value allowed by the corresponding theory or certain observation information in order for the predictions to be meaningful. This means that the corresponding upper limit of  $\kappa$  can add additional information to access the reliability of  $\kappa$  value obtained by observational constraints. Furthermore, studying the apparent EOS of actual compact stars such NS and QS could complement the previous results and shade more light on the understanding of gravitational matter coupling [1].

In this work, we investigate the role of the compactness extracted from recent the masses and radii of the same pulsars from Ref. [42]. Interestingly the corresponding compactness range is not much different from the range extracted by using the combination of recent masses and radii of pulsars from Refs.[43–45]. Note that the causality limit taken from

Ref [45] is used as an additional constraint. These observations are used to obtain the upper limit of NS and QS  $\kappa$ . We also investigate the compatibility of the NS and QS apparent EOSs with energy conditions up to a quite wide range of  $\kappa$  values.

The EOS of the NS core is calculated by using the relativistic mean field model with BSP parameter set [13] under which the standard SU(6) prescription and hyperon potential depths [46] are used to determine the hyperon coupling constants, while for the crust EOS the one proposed by Miyatsu *et al.* [47] is employed. Note indeed that the masses and the radius of NS or QS strongly depend on the adopted EOS. However, not all RMF parameter sets predictions are simultaneously compatible with the ones of pure neutron matter EOS at low density predicted by fundamental theory, experimental data of finite nuclei global properties, heavy ion experimental data predictions for symmetric nuclear matter and pure neutron matter EOSs at sub-saturation densities, etc. The BSP parameter set is one of the RMF parameter sets whose predictions pass all the corresponding tests (for example, see Refs. [13, 29] and references therein for more details about the features of EOS used in this work). Therefore, we use the BSP in this work as a representative parameter set with acceptable EOSs in quite a wide density range. We need also to note that in many works, if we consider that the hyperons should be present in order that we can obtain  $2 M_\odot$  predictions [43, 44] in GR, we should modify the standard prescriptions (see Refs [12, 13, 46] and references therein) to determine the hyperons coupling constants. For QS we used the EOS based on the confined-isospin-density-dependent-mass (CIDDM) model with additional vector Coulomb term of strange quark matter. This EOS also passes the test for acceptable EOS to describe the quark matter (see the details of the EOS in Ref. [14] and references therein). Note that the authors of Ref. [14] have found that within GR, if the Coulomb term is included, for the models where their parameters are consistent with SQM absolute stability condition, the  $2 M_\odot$  constraint prefers the maximum QS mass prediction of the model with the scalar Coulomb term to that of the model with the vector Coulomb term. See Ref. [14] for detail discussions of the role of Coulomb terms in the CIDDM model.

The paper is organized as follows. Sec. 2, describes briefly the formalism used in this work. Sec. 3 is devoted to discuss the results while the conclusion is given in Sec. 4.

## 2 Formalism

In this section, we shall briefly review the EiBI theory, by focusing more on the coupling of compact stars matter with gravity. Note that throughout this paper we use units  $c = G = 1$ , and in addition the parameter  $\kappa$  in this unit is  $(10^6 \text{m}^2)$  unit while in standard SI unit it becomes  $\kappa_g = 8 \pi G \kappa$  in  $\text{m}^5 \text{kg}^{-1} \text{s}^{-2}$  unit.

### 2.1 EiBI theory as GR with apparent EOS

We start from the action of EiBI theory of gravity given by [1, 27, 33]

$$S = \frac{1}{8\pi\kappa} \int d^4x \left( \sqrt{-|g_{\mu\nu} + \kappa R_{\mu\nu}|} - \lambda \sqrt{-g} \right) + S_M[g, \Psi_M], \quad (2.1)$$

where  $R_{\mu\nu}$  is the symmetric Ricci tensor. In the Palatini formalism  $R_{\mu\nu}$  is a functional of connection  $\Gamma_{\mu\nu}^\alpha$ ,  $R[\Gamma]$ , and the connection and the (physical) metric  $g_{\mu\nu}$  are treated as two independent fields. Meanwhile,  $\kappa$  and  $\lambda$  are parameters related to the Born-Infeld non-linearity and the cosmological constant, respectively. The action (2.1) reduces to the ordinary

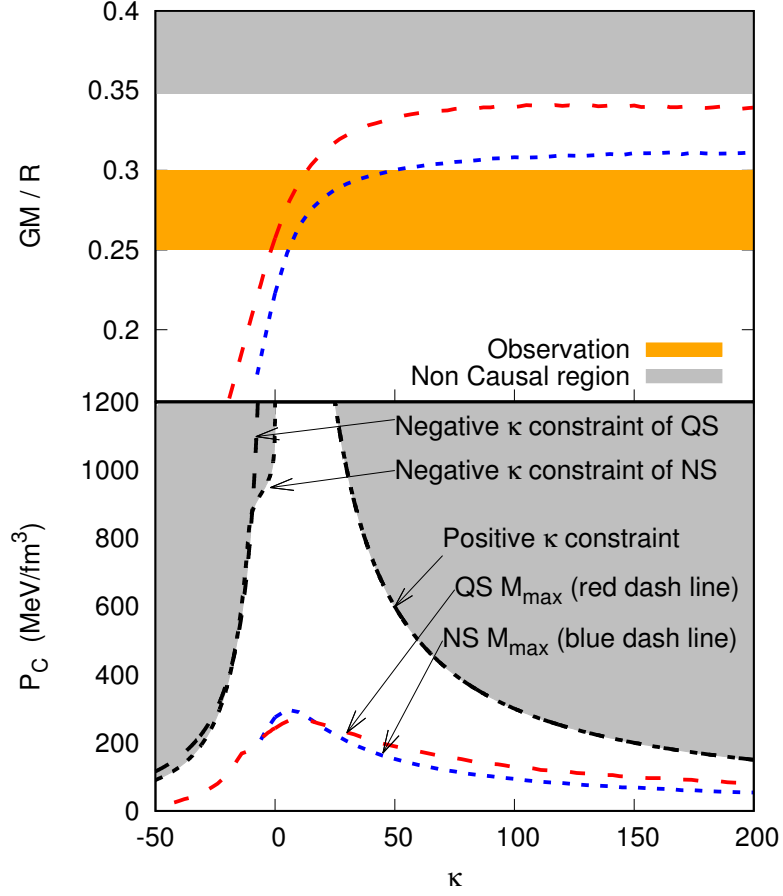


**Figure 1.** Compactness as a function of  $\kappa$  (upper panel), and central pressure as a function of  $\kappa$  (lower panel) plots. On the upper panel, non-causal region due to maximum compactness  $\simeq 0.35$  is taken from Ref.[45], while the constraint from observation data is taken from masses and radii data extracted from three known pulsars analysis of Ref.[42]. This compactness constraint is also compatible with one obtained from combination of masses from Ref.[43] and Ref.[44] and radii from Ref [45]. On the lower panel, the black dot and black-dash dot plots are generated based on the requirement that the value of  $\tau$  must be real and the corresponding constraint apply for both NS and QS, while the QS and NS  $M_{max}$  plots are the  $P_c$  and  $\kappa$  values which predict the corresponding maximum masses.

Einstein-Hilbert when  $\kappa \rightarrow 0$ . Here  $|g_{\mu\nu} + \kappa R_{\mu\nu}|$  denotes the absolute value of the determinant of the tensor  $(g_{\mu\nu} + \kappa R_{\mu\nu})$ .

Varying the action (2.1) with respect to  $\Gamma$  and  $g$ , we obtain the following equations:

$$\lambda q_{\mu\nu} = g_{\mu\nu} + \kappa R_{\mu\nu}, \quad (2.2)$$

$$q^{\mu\nu} = \tau (g^{\mu\nu} - 8\pi\kappa T^{\mu\nu}), \quad (2.3)$$

$$\Gamma_{\beta\gamma}^{\alpha} = \frac{1}{2} q^{\alpha\rho} (q_{\rho\beta,\gamma} + q_{\rho\gamma,\beta} - q_{\beta\gamma,\rho}), \quad (2.4)$$

where  $q_{\mu\nu}$  is the so-called “auxiliary” metric,  $\tau \equiv \sqrt{g/q}$ , and  $q$  is the determinant of metric  $q_{\mu\nu}$ .

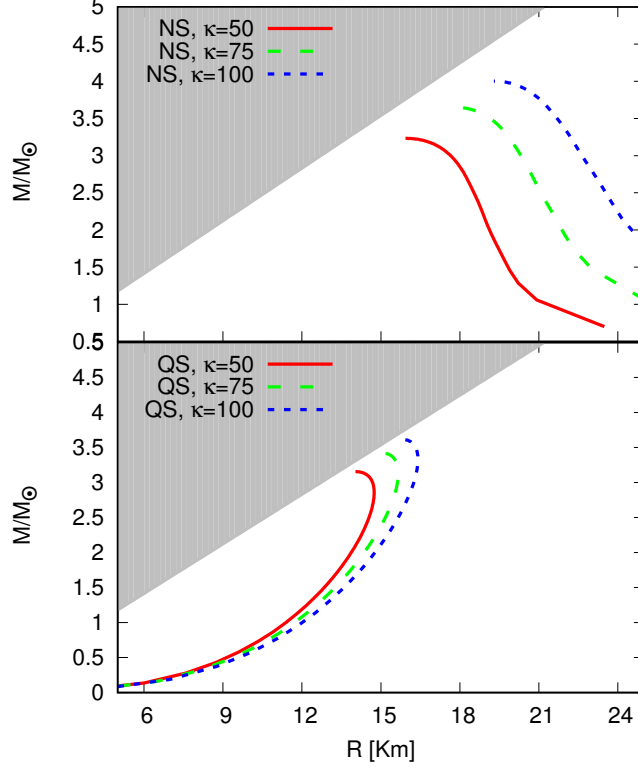


**Figure 2.** Mass-radius relation of NSs (upper panel) and QSs (lower panel) for large  $\kappa$  values. The gray-shaded area is non-causal region deduced from the critical compactness  $\frac{GM}{R} \simeq 0.35$  [45]. Each line represents the mass-radius relation for a particular value of  $\kappa$ .

From Eqs.(2.2) and (2.3), one can find the mixed Einstein tensor  $G_\nu^\mu$  for  $q_{\mu\nu}$  as (See Ref.[1] for details),

$$G_\nu^\mu[q_{\mu\nu}] \equiv R_\nu^\mu - \frac{1}{2}R\delta_\nu^\mu = 8\pi\mathcal{T}_\nu^\mu - \Lambda\delta_\nu^\mu,$$

with

$$\mathcal{T}_\nu^\mu \equiv \tau T_\nu^\mu + \left( \frac{\tau - 1 - 4\pi\tau\kappa T}{8\pi\kappa} \right) \delta_\nu^\mu, \quad (2.5)$$

and the cosmological constant  $\Lambda = (\lambda - 1)/\kappa$ . The function  $\tau$  can be obtained by multiplying Eq. (2.3) by metric  $g_{\nu\alpha}$  and then taking its determinant [1]

$$\tau = |(\delta_\nu^\mu - 8\pi\kappa T_\nu^\mu)|^{-\frac{1}{2}}. \quad (2.6)$$

Because it is assumed that the cosmological constant do not significantly influence the compact star properties, henceforth, we set  $\lambda \equiv 1$ .

The standard EOS model for compact stars is that the energy-momentum tensor assumes the form of perfect fluid, i.e.,

$$T_{\mu\nu} = (\epsilon + p)u_\mu u_\nu + pg_{\mu\nu}, \quad (2.7)$$

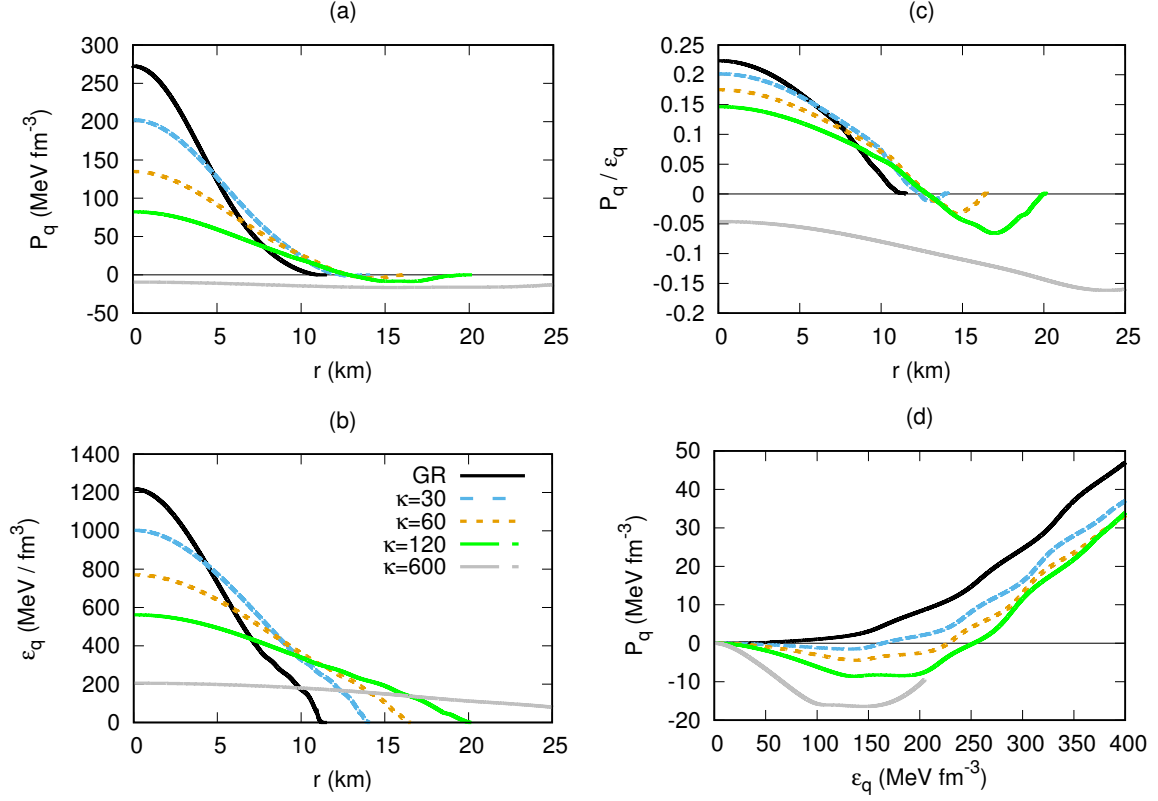


**Figure 3.** The profile for NSs with maximum mass. (a) The left-upper panel is the apparent pressure, (b) left-down panel is the apparent energy density, (c) right-upper panel is the ratio of pressure to energy density, and (d) right-down panel is the apparent EOS. Note that the apparent properties used in the plots are deducted from properties of maximum mass of NS for each  $\kappa$  value, as in Fig [1]

which satisfies the conservation equation,  $\nabla_\mu T^{\mu\nu} = 0$ . In Eq. (2.7),  $\epsilon$ ,  $p$ , and  $u_\mu$  denote the actual energy density, the isotropic pressure, and the four-velocity of the NS matter, respectively. It is shown in Ref. [1] that under this assumption, it is possible to re-express  $\mathcal{T}_\nu^\mu$  in the form of perfect fluid in terms of  $q_{\mu\alpha}$ , instead of  $g_{\mu\alpha}$ , with an apparent fluid velocity  $v^\mu$  obeys  $v^\mu v^\alpha q_{\mu\alpha} = -1$ , while the apparent pressure  $P_q$  and energy density  $\epsilon_q$  become

$$\begin{aligned} P_q &= \tau P + \mathcal{P} \\ \epsilon_q &= \tau \epsilon - \mathcal{P}, \end{aligned} \quad (2.8)$$

with

$$\begin{aligned} \mathcal{P} &\equiv \frac{\tau - 1 - 4\pi\tau\kappa(3P - \epsilon)}{8\pi\kappa}, \\ \tau &= [(1 + 8\pi\kappa\epsilon)(1 - 8\pi\kappa P)^3]^{-\frac{1}{2}}. \end{aligned} \quad (2.9)$$

It is obvious from Eq. (2.9) that in the limit of  $\kappa \rightarrow 0$ , then  $\mathcal{P} \rightarrow 0$  and  $\tau \rightarrow 1$ . From this view, EiBI becomes GR with additional isotropic gravitational pressure  $\mathcal{P}$  in apparent stress tensor  $\mathcal{T}_\nu^\mu$ . Here  $\tau$  should be real number and it depends on the actual EOS. The information of the difference between the apparent and actual EOS encodes in  $\tau$  and  $\mathcal{P}$ . We need to note

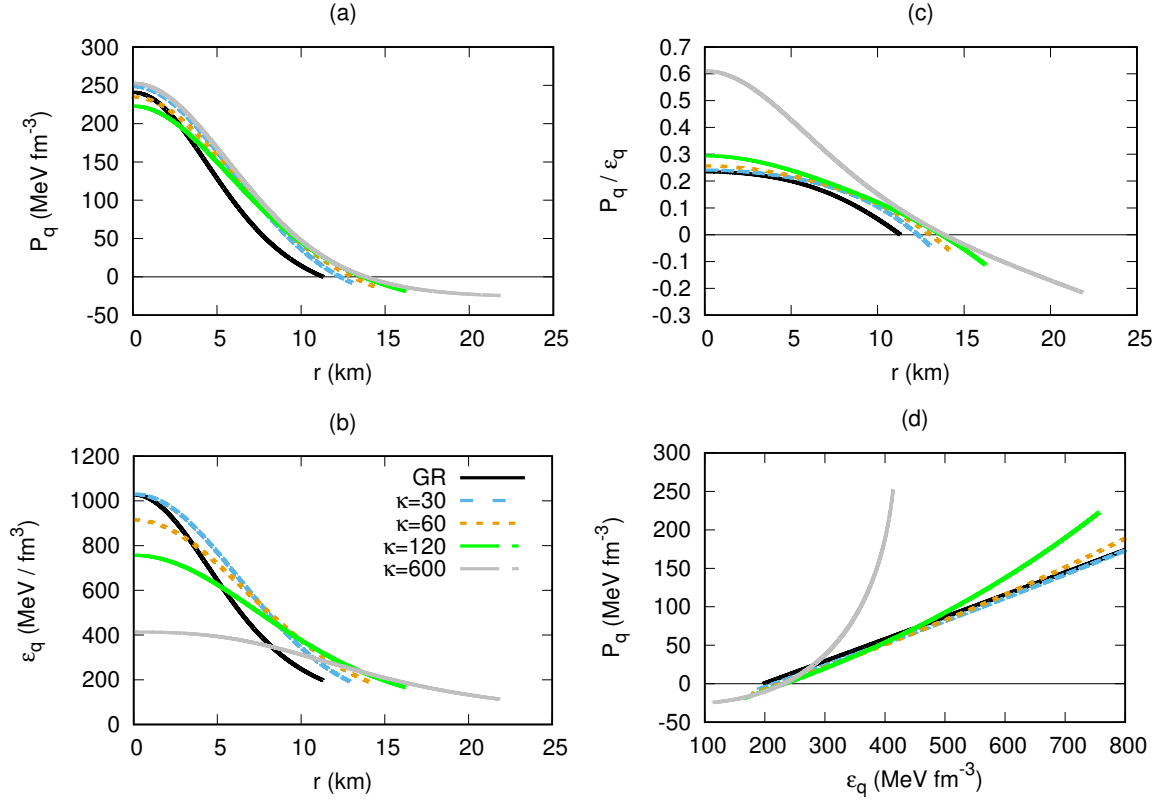


**Figure 4.** the profile for QSs with maximum mass. (a) The left-upper panel is the apparent pressure, (b) left-down panel is the apparent energy density, (c) right-upper panel is the ratio of pressure to energy density, and (d) right-down panel is the apparent EOS. Note that the apparent properties used in the plots are deducted from properties of maximum mass of QS for each  $\kappa$  value, as in Fig [1]

that in this point of view the NS observations such as mass-radius relations, quasi-normal mode, gravitational waves in general etc could be related also to the apparent EOS [1].

It is known that the acceptable EOS should satisfy the energy conditions. The corresponding energy conditions are [1]:

- null energy condition (NEC)

$$\epsilon + P \geq 0, \quad (2.10)$$

- weak energy condition (WEC)

$$\epsilon + P \geq 0, \text{ and } \epsilon \geq 0, \quad (2.11)$$

- strong energy condition (SEC)

$$\epsilon + P \geq 0, \text{ and } \epsilon + 3P \geq 0, \quad (2.12)$$

- dominant energy condition (DEC) and causal energy condition (CEC)

$$\epsilon \geq |P|, \text{ and } |\epsilon| \geq |P|. \quad (2.13)$$



We need also to point out that in order to be physically meaningful, the interior solution for static fluid spheres of GR must also satisfy some general physical requirements, such as (See Ref. [30] and the references therein for details):

- the density  $\epsilon$  and pressure  $p$  should be positive inside the star
- the gradients  $\frac{d\epsilon}{dr}$  and  $\frac{dp}{dr}$  should be negative,
- inside the static configuration the speed of sound should be less than the speed of light,
- the interior metric should be joined continuously with the exterior Schwarzschild metric,
- the pressure  $p$  must vanish at the boundary  $r = R$  of the sphere.

As mentioned previously, if we consider EiBI theory as GR with an apparent EOS, then the corresponding apparent EOS should obey those requirements. Therefore, we can investigate whether these NS matter requirements can constrain also  $\kappa$  from the predicted apparent EOS for NS and QS matters.

## 2.2 Compact stars in EiBI theory

Here we provide the TOV equations of EiBI theory version. The line element of the physical ( $g_{\mu\nu}$ ) and the auxiliary ( $q_{\mu\nu}$ ) metrics that describe the structure of compact static and spherically symmetric objects [33, 37] are

$$\begin{aligned} g_{\mu\nu}dx^\mu dx^\nu &= -e^{\nu(r)}c^2dt^2 + e^{\lambda(r)}dr^2 + f(r)d\Omega^2, \\ q_{\mu\nu}dx^\mu dx^\nu &= -e^{\beta(r)}c^2dt^2 + e^{\alpha(r)}dr^2 + r^2d\Omega^2. \end{aligned} \quad (2.14)$$

By using these definition for functions  $a$  and  $b$  as

$$a \equiv \sqrt{1 + 8\pi\kappa\epsilon}, \quad (2.15)$$

$$b \equiv \sqrt{1 - 8\pi\kappa P}, \quad (2.16)$$

we can obtain [29, 33]

$$m' = \frac{1}{4\kappa} \left( 2 + \frac{a}{b^3} - \frac{3}{ab} \right) r^2, \quad (2.17)$$

and a similar form as the one of GR, pressure derivative, can also be obtained as

$$P' = -\frac{b}{4\pi\kappa} \frac{ab(a^2 - b^2) \left( \frac{1}{2\kappa} \left( \frac{1}{ab} + \frac{a}{b^3} - 2 \right) r^3 + 2m \right)}{r^2 (1 - 2m) [4ab^2 + (3a - bc_q^2)(a^2 - b^2)]}, \quad (2.18)$$

where  $c_q^2 = \left( \frac{da(b)}{db} \right) = -\frac{b}{a} \left( \frac{d\epsilon}{dp} \right)$  and the prime in  $p$  and  $m$  in Eqs. (2.17) and (2.18) means the first derivative of the corresponding variables in respect to  $r$ . We need to note that EiBI and GR theories are identical for the region outside the star ( $r \geq R$ ). Therefore, we can use the same boundary conditions at  $r = R$  as those of GR for solving TOV equations. In the end, we can obtain static properties of compact stars based on the EiBI theory of gravity by explicitly solving Eqs. (2.17) and (2.18) using the corresponding EOS of NS [29] or QS [14] as an input.

### 3 Results and discussion

In the lower panel of Fig. 1, we show the allowed region of  $P_c$  and  $\kappa$  within the EiBI theory for NS and QS, respectively. The right and left gray-shaded regions are the excluded areas by the requirement that  $\tau \in \mathbb{R}$ . For positive  $\kappa$ , the right gray-shaded region is excluded by the  $P_c \leq \frac{1}{8\pi\kappa}$  constraint, and for negative  $\kappa$  the left gray-shaded region is excluded by the  $\epsilon_c \geq \frac{1}{8\pi\kappa}$  constraint. The difference of NS and QS for negative  $\kappa$  value close to 0 is due to the different composition of both stars, so that for the same  $P_c$  both stars have different  $\epsilon_c$ . These results are quite in-line with the ones reported in Ref. [1]. Each point in blue dot and red dash lines are obtained from the value of  $P_c$  and  $\kappa$  of NS and QS, with maximum masses, respectively. The region below these lines are the onset of stability regions of the NSs and QSs based on the EiBI theory. It is clear that the onset of stability regions of realistic model of the stars (NS and QS) exist inside the acceptable  $\kappa$  region from the one of the real  $\tau$  constraint. It also is interesting to observe that the stability condition for compact stars within EiBI constrains the maximum  $P_c$  instead of  $\kappa$  i.e., at  $P_c \approx 300 \text{ MeV fm}^{-3}$  and  $\kappa \approx 5$  ( $\kappa_g \approx 0.0083$ ) for NS and  $P_c \approx 270 \text{ MeV fm}^{-3}$  and  $\kappa \approx 12$  ( $\kappa_g \approx 0.020$ ) for QS. While the onset of stability for the corresponding stars is not too sensitive to the composition difference between NS and QS. The onset of stability of NS and QS is quite compatible with the one obtained from the relation  $\kappa\Delta < 0$  [26]. At certain negative value of  $\kappa$  i.e.,  $\kappa \approx -8$  ( $\kappa_g \approx -0.013$ ), the NS becomes unstable. This can be seen in the lower panel of Fig. 1 where the stability boundary line (blue-dashed line) of NS cannot be continued after reaching the negative value of  $\kappa$ . For the case of QS the value of the corresponding negative  $\kappa$  is significantly lower i.e.,  $\kappa \approx -50$  ( $\kappa_g \approx -0.084$ ). This could be due to the role of EOS crust in NS. The reason of the instability has been already discussed in Refs. [37, 41].

In the upper panel of Fig. 1, we show the maximum compactness as a function of  $\kappa$ . The gray-shaded area in the figure is the constraint from the region which is excluded by causality where the value of the compactness should be  $\lesssim 0.35$  [45]. For the constraint from observation, we take compactness value extracted from the data of three pulsars masses and radii analysis from Ref. [42]. It is expressed in the figure by the yellow-shaded area. It can be observed that the maximum compactness of the NS and QS stars saturate at large  $\kappa$  and they do not reach accusal region. It means that the EiBI stars have maximum compactness which is roughly independent on  $\kappa$ . This result is consistent with the one obtained by Ref.[26]. However, It can be observed also that the limit of maximum compactness of QS is closer to the accusal region compared to the one of NS. The compactness constraint from the observational data of Refs. [42] can be used as restricted constraints for the upper limit of  $\kappa$ . Here we obtain  $\kappa \lesssim 13$  ( $\kappa_g \lesssim 0.022$ ) for QS and  $\kappa \lesssim 47$  ( $\kappa_g \lesssim 0.079$ ) for NS. Note that Ref. [29] used  $2 M_\odot$  to obtain lower limit of  $\kappa$  for NS i.e.,  $4 \lesssim \kappa \lesssim 6$  or  $0.006 \lesssim \kappa_g \lesssim 0.01$ . Refs. [25, 32] obtained  $|\kappa_g| \lesssim 0.01$  for NS. It is reported in [34] that the sun properties can be used to constrain  $\kappa$ , that  $|\kappa_g| \lesssim 3 \times 10^5$ . This constraint is significantly looser than the ones of NS upper limit  $\kappa_g$ . If the saturation of energy density  $\epsilon_0 = 2.68 \times 10^{14} \text{ g cm}^{-2}$  the authors of Ref.[25] reported that moment of inertia of NS expected from the future observation can be estimated about  $|8\pi\kappa_g\epsilon_0| \lesssim 0.1$ . It was also shown in Ref. [31] that one could distinguish EiBI with  $8\pi\kappa_g\epsilon_0 \lesssim 0.03$  from GR from fundamental frequency of stellar oscillation, independent of the EOS for NS matter.

The result in the upper panel of Fig. 1 is consistent with the mass-radius relations shown in Fig. 2. It can be seen in the upper panel of Fig. 1 that as the value of  $\kappa$  increases the maximum mass and the corresponding radius do also increase. It causes the compactness

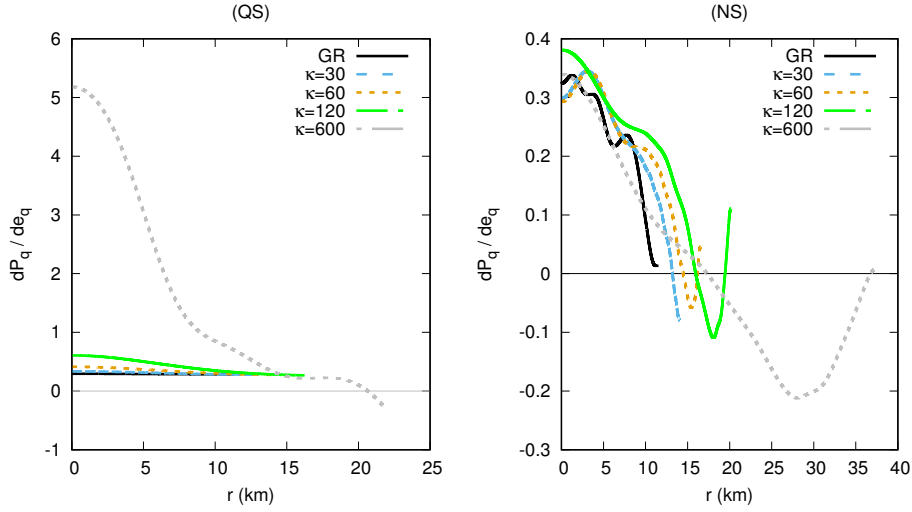


**Figure 5.** The apparent sound speed for NS in the right panel, and for QS in the left panel.

to increase up to a certain point at high  $\kappa$  value, then it saturates. Therefore, the causality restriction region in Fig. 2 can always be avoided for both compact stars. In addition it is shown in the lower panel of Fig. 2 that QS within CIDDm with vector Coulomb term EOS can also achieve higher maximum mass with larger  $\kappa$  value. It means that the vector-model of QS can also achieve maximum mass higher than  $2.0 M_{\odot}$ . This maximum mass cannot be achieved if one uses standard GR in the QS calculation within the CIDDm with vector-Coulomb term in the EOS [14].

In the following we will discuss the compatibility of the apparent EOS of NS and QS within the EiBI theory with constraint from energy conditions. The simultaneous fulfillment of the energy conditions of Eqs. (2.10-2.13) can be synthesized and observed from the relations:  $\epsilon \geq 0$ , and  $\frac{P}{\epsilon} \geq -\frac{1}{3}$ , with  $|P| \leq \epsilon$ . Furthermore, the fulfillment of corresponding energy conditions for the apparent EOSs of realistic models of NS and QS can be observed clearly from the profile of maximum masses shown in Fig. 3 for NSs and Fig. 4 for QSs. It can be seen in the left-lower panel of Fig. 3 and Fig. 4 that the apparent energy densities of NSs and QSs still have positive value everywhere ( $\epsilon_q \geq 0$ ). The right-upper panel of Fig. 3 and Fig. 4 show the ratio value of apparent pressure to apparent energy condition  $\frac{P_q}{\epsilon_q}$ . We expect by observing the change of trend due to the varying  $\kappa$  value in upper right panel of Fig. 3 and Fig. 4, that at a very large  $\kappa$  value the apparent EOSs will eventually violate the tighter SEC, namely  $\frac{P_q}{\epsilon_q} \geq -\frac{1}{3}$ . However, even up to the value of  $\kappa = 600$  ( $\kappa_9 = 1$ ) the corresponding constraint is still not saturated. It means that if our expectation is right, this energy condition will be violated only at the extremely large  $\kappa$ . In the upper panels of Fig. 3, one can observe that the apparent pressure of NSs becomes negative in the region close to the surface (crust) of the stars. The effect becomes larger if higher  $\kappa$  is used in the calculation. Similar situation happens in QSs (upper panels of Fig. 4), where the apparent pressure becomes negative in the region close to the surface of the stars. It is interesting to observe that the apparent pressure of QS is not going to be zero at the surface edge, while the NS goes back to zero there. This happens because NSs have a crust while QSs do not. Note that on the NS crust the EOS has a different structure compared to the one at the core. However, if we compare the apparent EOS profile of maximum mass of NS with the one of QS at a very large  $\kappa$ ,

the behavior is significantly different. The apparent pressure of NS at  $\kappa = 600$  ( $\kappa_g = 1.0$ ), for example, becomes negative from the center of NS until the surface, while the negative apparent pressure in the center starts to appear at  $\kappa \simeq 460$  ( $\kappa_g \simeq 0.77$ ). On the other hand, in QS the negative apparent pressure appears only on the surface. Note that the actual EOS coincide with the apparent EOS in the case of GR (black line) and the actual EOS satisfies all of the energy conditions. Furthermore, the actual EOS has only positive pressure value everywhere. Therefore, from the results in Fig. 3 and Fig. 4, we can conclude that up to quite a wide range of  $\kappa$  the apparent EOS for NSs and QSs satisfy all of the energy conditions simultaneously. On the other hand, if we observe that for NS with  $\kappa \leq 47$  ( $\kappa_g \leq 0.079$ ) at the surface the maximum  $|P_q| \lesssim 1 \text{ MeV fm}^{-3}$ , while for QS with  $\kappa \leq 13$  ( $\kappa_g \leq 0.022$ ) at the surface the maximum  $|P_q|$  is relative small i.e., more or less at the same order of magnitude with the one of NS. We can expect that for NSs with  $\kappa \leq 47$  ( $\kappa_g \leq 0.079$ ) and QSs with  $\kappa \leq 13$  ( $\kappa_g \leq 0.022$ ) within EiBI, the corresponding EOSs do not significantly violate the general physical EOS requirement for acceptable interior solution for static fluid spheres of GR i.e., the requirement that  $P_q$  should be positive inside the star. Unfortunately it is not really the case. We show the profiles of square of the apparent sound of speed for NS and QS maximum masses in Fig. 5 to see the impact of the appearance of negative value  $P_q$  in the region close to surface. It can be seen in the left panel that in the QS case, the apparent squared sound of speed is still physically acceptable for  $\kappa \leq 120$  ( $\kappa_g \approx 0.20$ ), while for the case of NS (as shown in right panel) such value in the region close to the surface becomes negative if  $\kappa > 0$  and the corresponding absolute values becomes larger when  $\kappa$  increases. Note that for GR, the square of apparent sound of speed of NS or QS are always positive everywhere because  $P_q = P$ .

## 4 Conclusion

In this work, the compactness constraint of NSs and QSs are employed to investigate the upper limit of  $\kappa$  parameter in the EiBI theory. We also investigate the compatibility of the apparent EOSs of NS and QS with energy conditions as well as general physical requirement of static fluid spheres. For NS, the EOS of the star core is calculated using the relativistic mean field model with BSP parameter set [13] under which the standard SU(6) prescription and hyperon potential depths [46] are utilized to determine the hyperon coupling constants, while for the crust EOS the one proposed by Miyatsu *et al.* [47] is used. For QS we used EOS based on the CIDDMM model with additional vector Coulomb term of strange quark matter. We have found that for large  $\kappa$  value, both NS and QS do not exceed causality restrictions because the compactness of NS and QS is saturated after passing a certain large  $\kappa$  value. This finding is in agreement with the result obtained in Ref. [1]. The variation of  $\kappa$  causes the CIDDMM model with vector-Coulomb of QS reach the maximum mass  $\geq 2M_\odot$ . This happens because a large value of  $\kappa$  can yield a large maximum mass value of QS compared to that of GR. This results complement the results found in Ref.[14]. The apparent EOS of NSs and QSs with wide range of  $\kappa$  can satisfy the energy conditions constraints. It is indicated that for extreme large value of  $\kappa$ , the strong energy condition can be violated. The fraction of  $\frac{P_q}{\epsilon_q}$  will be less than  $-\frac{1}{3}$  in such extremely large of value of  $\kappa$ . The general physical EOS requirement for acceptable interior solution for static fluid spheres of GR can be also violated by apparent EOS. In the NSs case, the square of the speed of sound of the corresponding apparent EOSs in the region near the NS surface becomes negative. To this end, from compactness and energy conditions analysis we conclude that the upper limit of  $\kappa$  value of NS is  $\kappa \approx 47$  ( $\kappa_g \approx 0.079$ ).

This results complement the constraints of  $\kappa$  value of NS result obtained by the authors in Refs. [25, 29, 32]. Furthermore, we also obtain that the upper limit of  $\kappa$  value of QS within CIDD model with additional vector Coulomb term is  $\kappa \approx 13$  ( $\kappa_g \approx 0.022$ ).

## ACKNOWLEDGMENT

We thank Ilham Prasetyo for useful discussions during the course of this work. AS is partially supported by the UI's PITTA grant No. 622/UN2.R3.1/HKP.05.00/2017. HSR is partially supported by the UI's PITTA grant No. 656/UN2.R3.1/HKP.05.00/2017.

## References

- [1] T. Delsate and J. Steinhoff, “New insights on the matter-gravity coupling paradigm,” *Phys. Rev. Lett.* **109** (2012) 021101 [arXiv:1201.4989 [gr-qc]].
- [2] E. Berti *et al.*, “Testing General Relativity with Present and Future Astrophysical Observations,” *Class. Quant. Grav.* **32** (2015) 243001 [arXiv:1501.07274 [gr-qc]].
- [3] C. M. Will, “The Confrontation between General Relativity and Experiment,” *Living Rev. Rel.* **17** (2014) 4 [arXiv:1403.7377 [gr-qc]].
- [4] D. Psaltis, “Probes and Tests of Strong-Field Gravity with Observations in the Electromagnetic Spectrum,” *Living Rev. Rel.* **11** (2008) 9 [arXiv:0806.1531 [astro-ph]].
- [5] K. Y. Eksi, C. Gungor and M. M. Turkoglu, “What does a measurement of mass and/or radius of a neutron star constrain: Equation of state or gravity?,” *Phys. Rev. D* **89** (2014) no.6, 063003 [arXiv:1402.0488 [astro-ph.HE]].
- [6] S. DeDeo and D. Psaltis, “Towards New Tests of Strong-field Gravity with Measurements of Surface Atomic Line Redshifts from Neutron Stars,” *Phys. Rev. Lett.* **90** (2003) 141101 [astro-ph/0302095].
- [7] J. M. Lattimer, “The nuclear equation of state and neutron star masses,” *Ann. Rev. Nucl. Part. Sci.* **62** (2012) 485 [arXiv:1305.3510 [nucl-th]].
- [8] N. Chamel, P. Haensel, J. L. Zdunik and A. F. Fantina, “On the Maximum Mass of Neutron Stars,” *Int. J. Mod. Phys. E* **22** (2013) 1330018 [arXiv:1307.3995 [astro-ph.HE]].
- [9] D. Lonardoni, A. Lovato, S. Gandolfi and F. Pederiva, “Hyperon Puzzle: Hints from Quantum Monte Carlo Calculations,” *Phys. Rev. Lett.* **114** (2015) no.9, 092301 [arXiv:1407.4448 [nucl-th]].
- [10] Y. Yamamoto, T. Furumoto, N. Yasutake and T. A. Rijken, “Hyperon mixing and universal many-body repulsion in neutron stars,” *Phys. Rev. C* **90** (2014) 045805 [arXiv:1406.4332 [nucl-th]].
- [11] A. V. Astashenok, S. Capozziello and S. D. Odintsov, “Maximal neutron star mass and the resolution of the hyperon puzzle in modified gravity,” *Phys. Rev. D* **89** (2014) no.10, 103509 [arXiv:1401.4546 [gr-qc]].
- [12] S. Weissenborn, I. Sagert, G. Pagliara, M. Hempel and J. Schaffner-Bielich, “Quark Matter In Massive Neutron Stars,” *Astrophys. J.* **740** (2011) L14 [arXiv:1102.2869 [astro-ph.HE]].
- [13] A. Sulaksono and B. K. Agrawal, “Existence of hyperons in the pulsar PSRJ1614-2230,” *Nucl. Phys. A* **895** (2012) 44 [arXiv:1209.6160 [nucl-th]].
- [14] A. I. Qauli and A. Sulaksono, “Quark matter at high density based on an extended confined isospin-density-dependent mass model,” *Phys. Rev. D* **93** (2016) no.2, 025022 [arXiv:1605.01154 [nucl-th]].

- [15] E. Farhi and R. L. Jaffe, “Strange Matter,” *Phys. Rev. D* **30** (1984) 2379; M. S. Berger and R. L. Jaffe, “Radioactivity in strange quark matter,” *Phys. Rev. C* **35** (1987) 213; E. P. Gilson and R. L. Jaffe, “Very small strangelets,” *Phys. Rev. Lett.* **71** (1993) 332 [[hep-ph/9302270](#)].
- [16] P. C. Chu and L. W. Chen, “Quark matter symmetry energy and quark stars,” *Astrophys. J.* **780** (2014) 135 [[arXiv:1212.1388 \[astro-ph.SR\]](#)].
- [17] P. Rehberg, S. P. Klevansky and J. Hufner, “Hadronization in the SU(3) Nambu-Jona-Lasinio model,” *Phys. Rev. C* **53** (1996) 410 [[hep-ph/9506436](#)]; M. Hanauske, L. M. Satarov, I. N. Mishustin, H. Stoecker and W. Greiner, “Strange quark stars within the Nambu-Jona-Lasinio model,” *Phys. Rev. D* **64** (2001) 043005 [[astro-ph/0101267](#)]; S. B. Ruester and D. H. Rischke, “Effect of color superconductivity on the mass and radius of a quark star,” *Phys. Rev. D* **69** (2004) 045011 [[nucl-th/0309022](#)]; D. Peres Menezes, C. Providencia and D. B. Melrose, “Quark stars within relativistic models,” *J. Phys. G* **32** (2006) 1081 [[astro-ph/0507529](#)].
- [18] C. D. Roberts and A. G. Williams, “Dyson-Schwinger equations and their application to hadronic physics,” *Prog. Part. Nucl. Phys.* **33** (1994) 477 [[hep-ph/9403224](#)]; H. S. Zong, L. Chang, F. Y. Hou, W. M. Sun and Y. X. Liu, “New approach for calculating the dressed quark propagator at finite chemical potential,” *Phys. Rev. C* **71** (2005) 015205; S. x. Qin, L. Chang, H. Chen, Y. x. Liu and C. D. Roberts, “Phase diagram and critical endpoint for strongly-interacting quarks,” *Phys. Rev. Lett.* **106** (2011) 172301 [[arXiv:1011.2876 \[nucl-th\]](#)].
- [19] A. Kurkela, P. Romatschke and A. Vuorinen, “Cold Quark Matter,” *Phys. Rev. D* **81** (2010) 105021 [[arXiv:0912.1856 \[hep-ph\]](#)].
- [20] M. Alford, M. Braby, M. W. Paris and S. Reddy, “Hybrid stars that masquerade as neutron stars,” *Astrophys. J.* **629** (2005) 969 [[nucl-th/0411016](#)]; K. Masuda, T. Hatsuda and T. Takatsuka, “Hadron-Quark Crossover and Massive Hybrid Stars with Strangeness,” *Astrophys. J.* **764** (2013) 12 [[arXiv:1205.3621 \[nucl-th\]](#)].
- [21] K. Yagi and N. Yunes, “I-Love-Q,” *Science* **341** (2013) 365 [[arXiv:1302.4499 \[gr-qc\]](#)].
- [22] G. Pappas and T. A. Apostolatos, “Effectively universal behavior of rotating neutron stars in general relativity makes them even simpler than their Newtonian counterparts,” *Phys. Rev. Lett.* **112** (2014) 121101 [[arXiv:1311.5508 \[gr-qc\]](#)].
- [23] K. Yagi, K. Kyutoku, G. Pappas, N. Yunes and T. A. Apostolatos, “Effective No-Hair Relations for Neutron Stars and Quark Stars: Relativistic Results,” *Phys. Rev. D* **89** (2014) no.12, 124013 [[arXiv:1403.6243 \[gr-qc\]](#)].
- [24] J. Beltran Jimenez, L. Heisenberg, G. J. Olmo and D. Rubiera-Garcia, “Born-Infeld inspired modifications of gravity,” [arXiv:1704.03351 \[gr-qc\]](#).
- [25] P. Pani, V. Cardoso and T. Delsate, “Compact stars in Eddington inspired gravity,” *Phys. Rev. Lett.* **107** (2011) 031101 [[arXiv:1106.3569 \[gr-qc\]](#)].
- [26] P. Pani, T. Delsate and V. Cardoso, “Eddington-inspired Born-Infeld gravity. Phenomenology of non-linear gravity-matter coupling,” *Phys. Rev. D* **85** (2012) 084020 [[arXiv:1201.2814 \[gr-qc\]](#)].
- [27] M. Banados and P. G. Ferreira, “Eddington’s theory of gravity and its progeny,” *Phys. Rev. Lett.* **105** (2010) 011101 Erratum: [*Phys. Rev. Lett.* **113** (2014) no.11, 119901] [[arXiv:1006.1769 \[astro-ph.CO\]](#)].
- [28] M. Born and L. Infeld, “Foundations of the new field theory,” *Proc. Roy. Soc. Lond. A* **144** (1934) 425.
- [29] A. I. Qauli, M. Iqbal, A. Sulaksono and H. S. Ramadhan, “Hyperons in neutron stars within an Eddington-inspired Born-Infeld theory of gravity,” *Phys. Rev. D* **93** (2016) no.10, 104056 [[arXiv:1605.01152 \[astro-ph.SR\]](#)].

- [30] M. K. Mak and T. Harko, “Isotropic stars in general relativity,” *Eur. Phys. J. C* **73** (2013) 2585 [arXiv:1309.5123 [gr-qc]].
- [31] H. Sotani, “Observational discrimination of Eddington-inspired Born-Infeld gravity from general relativity,” *Phys. Rev. D* **89** (2014) no.10, 104005 [arXiv:1404.5369 [astro-ph.HE]].
- [32] P. P. Avelino, “Eddington-inspired Born-Infeld gravity: astrophysical and cosmological constraints,” *Phys. Rev. D* **85** (2012) 104053 [arXiv:1201.2544 [astro-ph.CO]].
- [33] T. Harko, F. S. N. Lobo, M. K. Mak and S. V. Sushkov, “Structure of neutron, quark and exotic stars in Eddington-inspired Born-Infeld gravity,” *Phys. Rev. D* **88** (2013) 044032 [arXiv:1305.6770 [gr-qc]].
- [34] J. Casanellas, P. Pani, I. Lopes and V. Cardoso, “Testing alternative theories of gravity using the Sun,” *Astrophys. J.* **745** (2012) 15 [arXiv:1109.0249 [astro-ph.SR]].
- [35] H. Sotani, “Stellar oscillations in Eddington-inspired Born-Infeld gravity,” *Phys. Rev. D* **89** (2014) no.12, 124037 [arXiv:1406.3097 [astro-ph.HE]].
- [36] Y.-H. Sham, L.-M. Lin and P. T. Leung, “Radial oscillations and stability of compact stars in Eddington inspired Born-Infeld gravity,” *Phys. Rev. D* **86** (2012) 064015 [arXiv:1208.1314 [gr-qc]].
- [37] Y. H. Sham, P. T. Leung and L. M. Lin, “Compact stars in Eddington-inspired Born-Infeld gravity: Anomalies associated with phase transitions,” *Phys. Rev. D* **87** (2013) no.6, 061503 [arXiv:1304.0550 [gr-qc]].
- [38] E. Barausse, T. P. Sotiriou and J. C. Miller, “A No-go theorem for polytropic spheres in Palatini  $f(R)$  gravity,” *Class. Quant. Grav.* **25** (2008) 062001 [gr-qc/0703132 [GR-QC]].
- [39] P. Pani and T. P. Sotiriou, “Surface singularities in Eddington-inspired Born-Infeld gravity,” *Phys. Rev. Lett.* **109** (2012) 251102 [arXiv:1209.2972 [gr-qc]].
- [40] P. Pani, T. P. Sotiriou and D. Vernieri, “Gravity with Auxiliary Fields,” *Phys. Rev. D* **88** (2013) no.12, 121502 [arXiv:1306.1835 [gr-qc]].
- [41] H. C. Kim, “Physics at the surface of a star in Eddington-inspired Born-Infeld gravity,” *Phys. Rev. D* **89** (2014) no.6, 064001 [arXiv:1312.0705 [gr-qc]].
- [42] F. Ozel and P. Freire, “Masses, Radii, and Equation of State of Neutron Stars,” *Ann. Rev. Astron. Astrophys.* **54** (2016) 401 [arXiv:1603.02698 [astro-ph.HE]].
- [43] J. Antoniadis *et al.*, “A Massive Pulsar in a Compact Relativistic Binary,” *Science* **340** (2013) 6131 [arXiv:1304.6875 [astro-ph.HE]].
- [44] A. W. Steiner, J. M. Lattimer and E. F. Brown, “The Equation of State from Observed Masses and Radii of Neutron Stars,” *Astrophys. J.* **722** (2010) 33 [arXiv:1005.0811 [astro-ph.HE]].
- [45] J. M. Lattimer and M. Prakash, “Neutron Star Observations: Prognosis for Equation of State Constraints,” *Phys. Rept.* **442** (2007) 109 [astro-ph/0612440].
- [46] J. Schaffner-Bielich and A. Gal, “Properties of strange hadronic matter in bulk and in finite systems,” *Phys. Rev. C* **62** (2000) 034311 [nucl-th/0005060].
- [47] T. Miyatsu, S. Yamamuro and K. Nakazato, “A new equation of state for neutron star matter with nuclei in the crust and hyperons in the core,” *Astrophys. J.* **777** (2013) 4 [arXiv:1308.6121 [astro-ph.HE]].